Adaptive Observer-Based Sliding Mode Secure Control for Nonlinear Descriptor Systems Against Deception Attacks

M. Kchaou[1], L Ladhar[2], M Omri[3], R. Abbassi[4], H. Jerbi[5]
College of Engineering University of Hail, Hail, Saudi Arabia[1,4,5]
Department of Electrical and Computer Engineering-Faculty of Engineering,
King Abdul Aziz University, Jeddah 21589, Saudi Arabia[2]
Deanship of Scientific Research (DSR), King Abdulaziz University, Jeddah 21589, Saudi Arabia[3]

***Abstract*—This paper delves into an advanced control scheme that combines the sliding mode control (SMC) strategy with a meta-heuristic method to examine the issue of security control for non-linear systems that are vulnerable to deception attacks on their sensors and actuators. The proposed approach focuses on the development of a secure SMC law for nonlinear descriptor systems described by TS fuzzy models. A fuzzy observer is designed to accurately estimate the states that may affected by unpredictable sensor attacks, and an adaptive SMC controller is synthesized based on the estimated information to drive the observer's state trajectories towards the sliding surface and then maintaining the sliding motion thereafter. Afterward, sufficient conditions are established to ensure the admissibility of the closed-loop system. Then, the secretary bird optimization algorithm (SBOA), is explored for tackling an optimization problem with non-convex and nonlinear constraints as is defined to enhance the system's performance under threats. Ultimately, a simulation study through a practical example is performed to showcase the effectiveness of the proposed control scheme in maintaining system performance, even in the presence of attacks.**

***Keywords*—Descriptor systems; TS fuzzy models; fuzzy observer; deception attacks; adaptive sliding mode; SBOA**

I. Introduction

Exploring non-linear systems has always been an important topic in both the theoretical and practical aspects of control engineering. In this regard, fuzzy logic theory has emerged as a promising approach to handling the synthesis of complex nonlinear systems. In particular, the TS fuzzy models have become increasingly popular as a viable solution for addressing nonlinear control and filtering design problems. Furthermore, owing to their distinctive characteristics, several academics have dedicated substantial effort and undertaken studies in recent decades [1], [2], [4], [5]. On the other hand, it is common knowledge that several physical plants have a particular mathematical description that includes algebraic constraints in their models. Referred to as the descriptor system, it is acknowledged that while exploiting this model, regularity and absence of impulse features must be examined [6], [7], [8], [9], [10]. Besides, there has been a significant amount of development in the area of cyber-physical systems (CPSs), which are focused on the combination of computing and physical resources. Smart grids and intelligent automobiles are two examples of industrial processes that heavily rely on these technology. However, adopting such a structure may present technical challenges in terms of system synthesis and security. In fact, malicious users may compromise CPSs' stability, confidentiality, and integrity by launching cyber attacks over wireless communications between sensors and controllers. Consequently, cyber-security has risen to the top of the list of priorities and is one of the most significant problems in the control community for developing feedback control systems that can withstand attacks [11]. When it comes to this topic, there are various classes of attacks that have drawn the attention of researchers: the denial-of-service (DoS) attacks examined in [12], [13], [21], and the deception attacks studied in [14], [15], [16]. DoS is unique in that the attacker sends a large number of meaningless signals to use up network bandwidth and confuse legitimate users requests were unable to pass through. However, deception attacks, unlike DoS, disrupt the system's information transmission process by injecting false data to destroy its authenticity and availability of information. Very recently, deception attacks have increasingly attracted a lot of attention from researchers, yielding a multitude of noteworthy findings (refer to [17], [18], [19], [14], [20]). To specify a few: The adaptive SMC approach has been explored in [13] to deal with the event-triggered control design for nonlinear systems with deception attacks. The study in [22] has focused on the secure event-triggered output feedback tracking control for singularly perturbed systems under sensor saturation and attack. In [33], the neural network is explored to deal with event-triggered control problem for Markov jump systems with DOS and deception attacks.

It should be emphasized that the aforementioned favorable findings only focused on attacks targeting the actuators or sensors. However, attacks affecting both sensor and actuator channels, which may occur often, should be seriously investigated. Besides, SMC is widely accepted as an exceptionally effective technique that exhibits rapid response and exceptional robustness against uncertainty and external disturbances [13], [23], [10], [24]. Thus, the SMC can be a valuable approach for dealing with security control issues in cyber-systems, especially when both the actuator and sensor are vulnerable to simultaneous attacks. Nevertheless, when the integrity of sensor signals is compromised, the system's state may be rendered inaccessible for controller design. On that account, it is necessary to construct an observer to estimate the unmeasured state in the event of a sensor attack [3]. Subsequently, the sliding mode controller should be synthesized based on the observer's estimation of the state. This fact serves as the primary motivation for our investigation. It should be mentioned that, as a result of attacks, the system's performance might be destroyed by unsuitable constructed SMC. To minimize the impact of the attacks, it is interesting to address an optimized SMC law by including an optimization problem that aims to optimize the controller and observer gains. To come up with nonlinear and non-convex constraints while designing the SM controller, the proposed problem cannot be addressed using the linear matrix inequality (LMI) approaches that are widely employed by scholars. Recently, several evolutionary algorithms, including the Genetic Algorithm (GA) [25], Particle Swarm Optimization (PSO) [26], the Ant Colony Optimization (ACO) [27], and the Dandelion Optimization (DO) [28], [29] have emerged to tackle design challenges in control systems that involve nonlinear or non-convex constraints. The population-based meta-heuristic algorithm SBOA, recently introduced in [39] will be used in conjunction with the LMI technique to address the problem of optimizing the control architecture. This serves as an additional incentive for this research.

This paper endeavors to design the observer-based sliding mode controller for a class of non-linear descriptor systems when both the actuator and sensor are vulnerable to attacks simultaneously. Compared with the existing works, the novelties of this paper lie in the following aspects:

- Although considerable attention has been devoted to standard state-space systems under attacks, the security control problem for descriptor systems (which naturally arise in many practical applications such as power systems, robotics, and process control) remains largely unexplored, especially when considering systems with nonlinear dynamics and fuzzy modeling.
- As compared to the existing findings [40], [41], the observer-based sliding mode secure problem for TS fuzzy descriptor systems is explored when both the actuator and sensor are vulnerable to attacks simultaneously.
- When sensor channels are compromised, traditional state-feedback controllers become impractical. Existing observer-based approaches for attacked systems [4], [28] primarily consider matched premise variables and do not address the optimization of both observer and controller gains to minimize attack amplification effects.
- Current SMC design methods for cyber-physical systems rely heavily on LMI approaches, which cannot handle the non-convex, nonlinear constraints that naturally arise when optimizing sliding surface parameters and controller gains to minimize attack impacts [40], [42], [36]. A new SBOA-assisted controller design method is schemed to mitigate the attack's effects and improve the system performance.

The remainder of this paper is organized as follows. Section II presents the system model and problem formulation, Section III establishes admissibility conditions through Lyapunov-based stability analysis. Section IV develops the synthesis of the adaptive sliding mode controller and derives the main theoretical contributions. Section V introduces the SBOA-based optimization problem used for optimal gain selection. Section VI validates the proposed approach through extensive simulation studies and comparative evaluations against existing methods. Finally, Section VII concludes the paper with suggestions for future research directions.

II. Preliminaries and Problem Statement

This section presents some preliminary concepts, and outlines the research problem.

A. Model Description

In this paper, the structure of control scheme is shown in Fig. 1, where the TS fuzzy model is employed to characterize nonlinear descriptor systems, where the following fuzzy rule is defined for the premise variables ϕ_j, $j \in \{1, \ldots, s\}$, and fuzzy sets $\mathbb{N}_j^i$, $i \in \mathbb{S} = \{1, \ldots, r\}$. r stands for the number of `if-then` rules.

Rule i: `if` ϕ_1 is $\mathbb{N}_1^i, \phi_2$ is $\mathbb{N}_2^i, \ldots,$ and ϕ_s is $\mathbb{N}_s^i$, `then`

$$\begin{cases} \boldsymbol{E}\dot{\boldsymbol{x}}(t) = \boldsymbol{A}_i\boldsymbol{x}(t) + \boldsymbol{B}_2\big(\boldsymbol{u}(t) + \boldsymbol{g}_i(t)\big), \\ \boldsymbol{y}(t) = \boldsymbol{C}_2\boldsymbol{x}(t) \end{cases} \tag{1}$$

In this model, $\boldsymbol{x}(t) \in \boldsymbol{R}^n$, $\boldsymbol{u}(t) \in \boldsymbol{R}^m$, and $\boldsymbol{y}(t) \in \boldsymbol{R}^{ny}$ define, respectively, the state vector, the control input, and the measured output. Matched non-linear function $\boldsymbol{g}_i(t)$ can represent various model uncertainties or external perturbations. Constant matrices $\boldsymbol{A}_i$, $\boldsymbol{B}_2$, $\boldsymbol{C}_2$, characterize the fuzzy model, matrix $\boldsymbol{E} \in \mathbb{R}^{n\times n}$, however, describes the singular property of the model so that $\text{rank}(\boldsymbol{E}) = r_0 < n$.

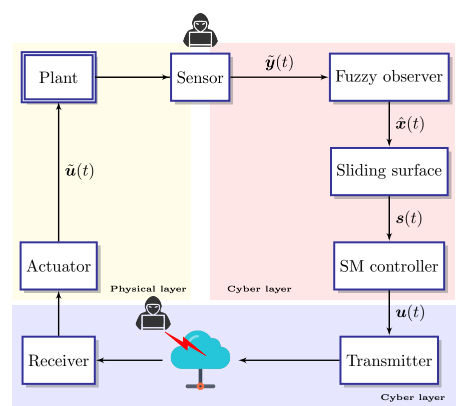

Fig. 1. Schematic of control structure.

B. Resulting Model

By identifying the vector $\boldsymbol{\phi} = [\phi_1, \ldots, \phi_s]$, the general fuzzy model is stated conform to:

$$\begin{cases} \boldsymbol{E}\dot{\boldsymbol{x}}(t) = \sum_{i=1}^{r} h_i(\boldsymbol{\phi})\Big\{\boldsymbol{A}_i(t)\boldsymbol{x}(t) + \boldsymbol{B}_2\big(\boldsymbol{u}(t) + \boldsymbol{g}_i(t)\big)\Big\}, \\ \boldsymbol{y}(t) = \boldsymbol{C}_2\boldsymbol{x}(t), \end{cases} \tag{2}$$

where $h_i(\boldsymbol{\phi}) = \prod_{j=1}^{\boldsymbol{s}} \mathcal{N}_j^i(\phi_j) / \sum_{i=1}^{r} \prod_{j=1}^{\boldsymbol{s}} \mathcal{N}_j^i(\phi_j)$ defines the normalized membership that should confirm $h_i(\boldsymbol{\phi}) \geq 0$, for $i \in \mathbb{S}$, and $\sum_{i=1}^{r} h_i(\phi) = 1$. $\mathcal{N}_j^i(\phi_j)$ stands for the grade of membership of ϕ_j to $\mathcal{N}_j^i$.

C. Attack's Descriptions

When the sensors are vulnerable to false data injection attacks caused by computer viruses, flaws, and similar factors, the following random model of the system outputs is investigated:

$$\tilde{\boldsymbol{y}}(t) = \boldsymbol{y}(t) + \zeta(t)(-\boldsymbol{y}(t) + \boldsymbol{\delta}_s(t)), \tag{3}$$

where $\zeta(t)$ is the random variable, while $\boldsymbol{\delta}_s(t)$ refers to the embedded signal produced by the attacker. It should be noted that, if $\zeta(t)$ is different from zero, then the sensor attack $\boldsymbol{\delta}_s(t)$ impacts the integrity of $\boldsymbol{y}(t)$; however, if $\zeta(t) = 0$, it comes $\tilde{\boldsymbol{y}}(t) = \boldsymbol{y}(t)$ which may be applied for feedback purposes. Again, through the injection of actuator attack signals, the integrity of $\boldsymbol{u}(t)$ is menaced and can be represented in the format that follows.

$$\tilde{\boldsymbol{u}}(t) = \boldsymbol{u}(t) + \boldsymbol{\delta}_a(t). \tag{4}$$

With (4), system (2) is expressed as

$$\begin{cases} \boldsymbol{E}\dot{\boldsymbol{x}}(t) = \boldsymbol{A}_h\boldsymbol{x}(t) + \boldsymbol{B}_2\big(\tilde{\boldsymbol{u}}(t) + \boldsymbol{g}_h(t)\big), \\ \quad \boldsymbol{y}(t) = \boldsymbol{C}_2\boldsymbol{x}(t), \end{cases} \tag{5}$$

and, the following norm bounded conditions hold for $\boldsymbol{g}_i(t)$, $\boldsymbol{\delta}_s(t)$, and $\boldsymbol{\delta}_a(t)$, respectively.

Assumption 1.

A.1 $\|\boldsymbol{g}_i(t)\| \leq \delta\|\boldsymbol{y}(t)\|$,

A.2 $\|\boldsymbol{\delta}_s(t))\| \leq \beta\|\boldsymbol{y}(t)\|$,

A.3 $\|\boldsymbol{\delta}_a(t))\| \leq \Theta\|\hat{\boldsymbol{x}}(t)\|$,

A.4 $\zeta(t)$ *is stochastic variable with a Bernoulli distribution characterized as* $Pr(\zeta(t) = 1) = \bar{\zeta}$, $Pr(\zeta(t) = 0) = 1 - \bar{\zeta}$.

where δ, β, Θ, *and* $\bar{\zeta}$ *are some known positive constants.*

D. Observer Design

It will underscored that sensor threats can compromise the accuracy of the output signal $\boldsymbol{y}(t)$ and complicate the process of designing state/output feedback controllers. Thus, an estimator should be designed to rebuild the system outputs. Under this circumstance, it is important to examine a fuzzy observer when faced with the challenge of mismatched premise variables between the observer and the system. The following rule states the model of the fuzzy observer, where $\boldsymbol{\varphi}(\hat{\boldsymbol{x}}(t)) = [\varphi_1(\hat{\boldsymbol{x}}(t)), \ldots, \varphi_{s_o}(\hat{\boldsymbol{x}}(t))]^\top$ is the premise variable vector that depends on the estimated states $\hat{\boldsymbol{x}}(t)$, and $\hat{\boldsymbol{y}}(t)$ depicts the estimated output.

Rule j: `if` $\varphi_1(\hat{\boldsymbol{x}}(t))$ is $\mathcal{V}_1^j, \ldots,$ and $\varphi_s(\hat{\boldsymbol{x}}(t))$ is $\mathcal{V}_{s_o}^j$, `then`

$$\begin{cases} \boldsymbol{E}\dot{\hat{\boldsymbol{x}}}(t) = \boldsymbol{A}_j\hat{\boldsymbol{x}}(t) + \boldsymbol{B}_2\tilde{\boldsymbol{u}}(t) + \boldsymbol{L}_j(\tilde{\boldsymbol{y}}(t) - \hat{\boldsymbol{y}}(t)), \\ \quad \hat{\boldsymbol{y}}(t) = \boldsymbol{C}_2\hat{\boldsymbol{x}}(t), \end{cases}$$

$\boldsymbol{L}_j$ is the observer gain to be determined. Accordingly, the global observer's dynamic is inferred as follows:

$$\begin{cases} \boldsymbol{E}\dot{\hat{\boldsymbol{x}}}(t) = \sum_{j=1}^{r} \mu_j(\boldsymbol{\varphi}(\hat{\boldsymbol{x}}))\Big(\boldsymbol{A}_j\hat{\boldsymbol{x}}(t) + \boldsymbol{B}_2\tilde{\boldsymbol{u}}(t) + \boldsymbol{L}_j(\tilde{\boldsymbol{y}}(t) - \hat{\boldsymbol{y}}(t))\Big), \\ \hat{\boldsymbol{y}}(t) = \boldsymbol{C}_2\hat{\boldsymbol{x}}(t), \end{cases} \tag{6}$$

where $\mu_j(\boldsymbol{\varphi}(\hat{\boldsymbol{x}}))$ is defined as $\mu_j(\boldsymbol{\varphi}(\hat{\boldsymbol{x}})) = \prod_{d_o=1}^{s_o} \mathcal{V}_{d_o}^j(\boldsymbol{\varphi}(\hat{\boldsymbol{x}})) \Big/ \sum_{j=1}^{r} \prod_{d_o=1}^{s_o} \mathcal{V}_{d_o}^j(\boldsymbol{\varphi}(\hat{\boldsymbol{x}})) \geq 0$, and satisfies $\sum_{j=1}^{r} \mu_j(\boldsymbol{\varphi}(\hat{\boldsymbol{x}})) = 1$. As well, the compact form of (6) being written as

$$\begin{cases} \boldsymbol{E}\dot{\hat{\boldsymbol{x}}}(t) &= \boldsymbol{A}_\mu\hat{\boldsymbol{x}}(t) + \boldsymbol{B}_2\tilde{\boldsymbol{u}}(t) + \boldsymbol{L}_\mu(\tilde{\boldsymbol{y}}(t) - \hat{\boldsymbol{y}}(t)), \\ \hat{\boldsymbol{y}}(t) &= \boldsymbol{C}_2\hat{\boldsymbol{x}}(t). \end{cases} \tag{7}$$

Let $\boldsymbol{e}(t) = \boldsymbol{x}(t) - \hat{\boldsymbol{x}}(t)$. The error dynamic system may be depicted as

$$\begin{aligned} \boldsymbol{E}\dot{\boldsymbol{e}}(t) =& (\boldsymbol{A}_h - \boldsymbol{A}_\mu + \bar{\zeta}\boldsymbol{L}_\mu\boldsymbol{C}_2)\hat{\boldsymbol{x}}(t) + \Big(\boldsymbol{A}_h - (1-\bar{\zeta})\boldsymbol{L}_\mu\boldsymbol{C}_2\Big)\boldsymbol{e}(t) \\ &+ \boldsymbol{B}_2\boldsymbol{g}_h(t) - \bar{\zeta}\boldsymbol{L}_\mu\boldsymbol{\delta}_s(t) - (\zeta(t) - \bar{\zeta})\boldsymbol{L}_\mu\boldsymbol{\Gamma}(t), \end{aligned} \tag{8}$$

where $\boldsymbol{\Gamma}(t) = -\boldsymbol{C}_2\hat{\boldsymbol{x}}(t) - \boldsymbol{C}_2\boldsymbol{e}(t) + \boldsymbol{\delta}_s(t)$.

E. Sliding Surfaces Design

When developing a sliding mode controller, it is crucial to establish a suitable switching function. This function should be defined and expressed in the following manner:

$$\boldsymbol{s}(t) = \bar{\boldsymbol{S}}\boldsymbol{E}(\hat{\boldsymbol{x}}(t) - \hat{\boldsymbol{x}}(0)) - \int_0^t \bar{\boldsymbol{S}}\Big(\boldsymbol{A}_\mu + \boldsymbol{B}_2\boldsymbol{K}_\mu\Big)\hat{\boldsymbol{x}}(\tau)d\tau, \tag{9}$$

Matrix $\bar{\boldsymbol{S}} \in \mathbb{R}^{m \times n}$ in (9) should be determined so that $\bar{\boldsymbol{S}}\boldsymbol{B}_2$ is non-singular. Moreover, as stated in the SMC theory, the ideal sliding mode occurs when $\boldsymbol{s}(t) = 0$ and $\dot{\boldsymbol{s}}(t) = 0$. Therefore, it may be inferred that

$$\begin{aligned} \dot{\boldsymbol{s}}(t) = \bar{\boldsymbol{S}}\boldsymbol{B}_2(\boldsymbol{u}(t) + \boldsymbol{\delta}_a(t) + \boldsymbol{g}_h(t) - \boldsymbol{K}_\mu\hat{\boldsymbol{x}}(t)) \\ + \bar{\boldsymbol{S}}\boldsymbol{L}_\mu(\tilde{\boldsymbol{y}}(t) - \hat{\boldsymbol{y}}(t)), \end{aligned} \tag{10}$$

and the equivalent control law is formally specified as:

$$\boldsymbol{u}_e(t) = \boldsymbol{K}_\mu\hat{\boldsymbol{x}}(t) - \boldsymbol{\delta}_a(t) - \boldsymbol{g}_h(t) - (\bar{\boldsymbol{S}}\boldsymbol{B}_2)^{-1}\bar{\boldsymbol{S}}\boldsymbol{L}_\mu(\tilde{\boldsymbol{y}}(t) - \hat{\boldsymbol{y}}(t)). \tag{11}$$

Moreover, the fuzzy sliding mode dynamics is defined as:

$$\begin{aligned} \boldsymbol{E}\dot{\hat{\boldsymbol{x}}}(t) = (\boldsymbol{A}_\mu + \boldsymbol{B}_2\boldsymbol{K}_\mu - \bar{\zeta}\hat{\boldsymbol{S}}\boldsymbol{L}_\mu\boldsymbol{C}_2)\hat{\boldsymbol{x}}(t) + (1-\bar{\zeta})\hat{\boldsymbol{S}}\boldsymbol{L}_\mu\boldsymbol{C}_2\boldsymbol{e}(t) \\ + \bar{\zeta}\hat{\boldsymbol{S}}\boldsymbol{L}_\mu\boldsymbol{\delta}_s(t) + (\zeta(t) - \bar{\zeta})\hat{\boldsymbol{S}}\boldsymbol{L}_\mu\boldsymbol{\Gamma}(t), \end{aligned} \tag{12}$$

where $\hat{\boldsymbol{S}} = \boldsymbol{I} - \tilde{\boldsymbol{S}}$, and $\tilde{\boldsymbol{S}} = \boldsymbol{B}_2(\bar{\boldsymbol{S}}\boldsymbol{B}_2)^{-1}\bar{\boldsymbol{S}}$.

Besides, the augmented closed-loop system can be characterized as:

$$\bar{\boldsymbol{E}}\dot{\bar{\boldsymbol{x}}}(t) = \bar{\boldsymbol{A}}_{h\mu}\bar{\boldsymbol{x}}(t) + \bar{\zeta}\bar{\boldsymbol{L}}_\mu\boldsymbol{\delta}_s(t) + \bar{\boldsymbol{B}}_2\boldsymbol{g}_h(t) + (\zeta(t) - \bar{\zeta})\bar{\boldsymbol{L}}_\mu\boldsymbol{\Gamma}(t), \tag{13}$$

where $\bar{\boldsymbol{x}}(t) = [\hat{\boldsymbol{x}}^\top(t), \boldsymbol{e}^\top(t)]^\top$,

$$\bar{\boldsymbol{E}} = \begin{bmatrix} \boldsymbol{E} & \boldsymbol{0} \\ \boldsymbol{0} & \boldsymbol{E} \end{bmatrix},$$
$$\bar{\boldsymbol{A}}_{h\mu} = \begin{bmatrix} \boldsymbol{A}_\mu - \bar{\zeta}\hat{\boldsymbol{S}}\boldsymbol{L}_\mu\boldsymbol{C}_2 + \boldsymbol{B}_2\boldsymbol{K}_\mu & (1-\bar{\zeta})\hat{\boldsymbol{S}}\boldsymbol{L}_\mu\boldsymbol{C}_2 \\ \boldsymbol{A}_h - \boldsymbol{A}_\mu + \bar{\zeta}\boldsymbol{L}_\mu\boldsymbol{C}_2 & \boldsymbol{A}_h - (1-\bar{\zeta})\boldsymbol{L}_\mu\boldsymbol{C}_2 \end{bmatrix},$$
$$\bar{\boldsymbol{L}}_\mu = \begin{bmatrix} \hat{\boldsymbol{S}}\boldsymbol{L}_\mu \\ -\boldsymbol{L}_\mu \end{bmatrix}, \bar{\boldsymbol{B}}_2 = \begin{bmatrix} \boldsymbol{0} \\ \boldsymbol{B}_2 \end{bmatrix}.$$

Remark 1. It is widely recognized that the sliding motion of the system is ensured when the matrix $\bar{\boldsymbol{S}}\boldsymbol{B}_2$ is non-singular. As stated in the literature, $\bar{\boldsymbol{S}}$ is often selected with a particular form, such as $\bar{\boldsymbol{S}}\boldsymbol{B}_2 = \boldsymbol{I}$ in [36], and $\bar{\boldsymbol{S}} = \boldsymbol{B}^\top\boldsymbol{P}$, where $\boldsymbol{P}$ is a positive definite Lyapunov matrix, as mentioned in [23]. However, selecting an unsuitable value for $\bar{\boldsymbol{S}}$ could result in the development of a SMC law that is ineffective in mitigating the effects of menaces. To address this concern, this study delves into a meta-heuristic approach for achieving the optimal selection of the sliding gain matrix $\bar{\boldsymbol{S}}$ and obtain the optimized SMC performance.

F. Objective Statements

The main objective of this study is to synthesize an adequate control that can effectively stabilize the system under investigation and successfully mitigate the negative effects of attacks $\boldsymbol{\delta}_s(t)$ and $\boldsymbol{\delta}_a(t)$. Hence, it is crucial to address the following questions to re-institute the ideal functionality of the controlled system.

Q-1 How may an adaptive sliding mode controller be designed to drive the observer states onto a pre-defined sliding surface and then maintaining the sliding motion thereafter?

Q-2 How may an optimization problem be formulated to minimize the effect of attacks and how can it be solved while dealing with non-convex constraints in the context of tackling the SMC problem?

Before responding to these questions, the following lemmas should be recalled.

Lemma 1. *[30] For any vectors $\boldsymbol{a}$, $\boldsymbol{b}$, and matrix $\boldsymbol{X} > 0$ the following inequality holds*

$$2\boldsymbol{a}^\top\boldsymbol{b} \leq \varsigma\boldsymbol{a}^\top\boldsymbol{X}\boldsymbol{a} + \varsigma^{-1}\boldsymbol{b}^\top\boldsymbol{X}\boldsymbol{b}, \tag{14}$$

for any scalar $\varsigma > 0$.

Lemma 2. *[31] The inequality $-\boldsymbol{Z} + \operatorname{sym}(\boldsymbol{Q}\boldsymbol{A}) < \boldsymbol{0}$ holds for appropriate dimension matrices $\boldsymbol{Z} > 0$, $\boldsymbol{Q}$, and $\boldsymbol{A}$ if the following condition is fulfilled for any constant $\lambda > 0$, and matrix $\boldsymbol{Y}$:*

$$\begin{bmatrix} -\boldsymbol{Z} & \boldsymbol{Q} + \lambda\boldsymbol{A}^\top\boldsymbol{Y}^\top \\ (\boldsymbol{Q} + \lambda\boldsymbol{A}^\top\boldsymbol{Y}^\top)^\top & -\lambda\operatorname{sym}(\boldsymbol{Y}) \end{bmatrix} < \boldsymbol{0}.$$

III. Admissibility Analysis

The development of sufficient conditions proving the stochastic admissibility of system (13) is the primary concern of this section.

Theorem 1. *Given positive scalars β, δ, and $\bar{\zeta}$. If there exists a set of scalar values $\tau, \alpha > 0$, together with matrices $\bar{\boldsymbol{P}} > 0$ and $\bar{\boldsymbol{N}}$, $\bar{\boldsymbol{M}}_1$ and $\bar{\boldsymbol{M}}_2$ that satisfy the following conditions:*

$$\sum_{i=1}^{r}\sum_{j=1}^{r} h_i(\boldsymbol{x})\mu_j(\hat{\boldsymbol{x}})\boldsymbol{\Phi}_{ij} < \boldsymbol{0}, \tag{15}$$

then, closed-loop system (13) is stochastically admissible.

$$\boldsymbol{\Phi}_{ij} = \begin{bmatrix} \boldsymbol{\Phi}_{11ij} & \boldsymbol{\Phi}_{12ij} & \bar{\zeta}\bar{\boldsymbol{M}}_1\bar{\boldsymbol{L}}_j & \bar{\boldsymbol{M}}_1\hat{\boldsymbol{B}}_2 \\ * & -\operatorname{sym}(\bar{\boldsymbol{M}}_2) & \bar{\zeta}\bar{\boldsymbol{M}}_2\bar{\boldsymbol{L}}_j & \bar{\boldsymbol{M}}_1\hat{\boldsymbol{B}}_2 \\ * & * & -\tau\boldsymbol{I} & \boldsymbol{0} \\ * & * & * & -\alpha\boldsymbol{I} \end{bmatrix}, \tag{16}$$

$\boldsymbol{\Phi}_{11ij} = \operatorname{sym}(\bar{\boldsymbol{M}}_1\bar{\boldsymbol{A}}_{ij}) + (\tau\beta^2 + \alpha\delta^2)\hat{\boldsymbol{C}}_2^\top\hat{\boldsymbol{C}}_2$, $\boldsymbol{\Phi}_{12ij} = \bar{\boldsymbol{E}}^\top\bar{\boldsymbol{P}} + \bar{\boldsymbol{N}}\bar{\boldsymbol{R}}^\top - \bar{\boldsymbol{M}}_1 + (\bar{\boldsymbol{M}}_2\bar{\boldsymbol{A}}_{ij})^\top$, $\hat{\boldsymbol{C}}_2 = \begin{bmatrix}\boldsymbol{C}_2 & \boldsymbol{C}_2\end{bmatrix}$, $\bar{\boldsymbol{R}}$ is any matrix satisfying $\bar{\boldsymbol{E}}^\top\bar{\boldsymbol{R}} = 0$ and $\operatorname{rank}(\bar{\boldsymbol{R}}) = 2n - 2r_0$.

Proof: First, we are concerned with the proof of the regularity and impulse-free features of (13). Suppose that non-singular matrices $\hat{\boldsymbol{V}}$, and $\hat{\boldsymbol{W}}$ exits so that $\hat{\boldsymbol{E}} = \hat{\boldsymbol{V}}\bar{\boldsymbol{E}}\hat{\boldsymbol{W}} = \operatorname{diag}\{\boldsymbol{I}_{2r_0}, \boldsymbol{0}\}$. Define

$$\hat{\boldsymbol{A}}_{h\mu} = \hat{\boldsymbol{V}}\bar{\boldsymbol{A}}_{h\mu}\hat{\boldsymbol{W}} = \begin{bmatrix} \hat{\boldsymbol{A}}_{11h\mu} & \hat{\boldsymbol{A}}_{12h\mu} \\ \hat{\boldsymbol{A}}_{21h\mu} & \hat{\boldsymbol{A}}_{22h\mu} \end{bmatrix}, \ \hat{\boldsymbol{N}} = \hat{\boldsymbol{W}}^\top\bar{\boldsymbol{N}} = \begin{bmatrix} \hat{\boldsymbol{N}}11 \\ \hat{\boldsymbol{N}}21 \end{bmatrix},$$
$$\hat{\boldsymbol{P}} = \hat{\boldsymbol{V}}^\top\bar{\boldsymbol{P}}\hat{\boldsymbol{V}} = \begin{bmatrix} \hat{\boldsymbol{P}}_{11} & \hat{\boldsymbol{P}}_{12} \\ * & \hat{\boldsymbol{P}}_{22} \end{bmatrix}, \hat{\boldsymbol{R}} = \hat{\boldsymbol{V}}^\top\bar{\boldsymbol{R}} = \hat{\boldsymbol{V}}^\top\begin{bmatrix} \hat{\boldsymbol{R}}_{11} \\ \hat{\boldsymbol{R}}_{21} \end{bmatrix}. \tag{17}$$

Using the fact that $\bar{\boldsymbol{E}}^\top\bar{\boldsymbol{R}} = \boldsymbol{0}$, if $\hat{\boldsymbol{R}}_{11} = \boldsymbol{0}$, it comes that $\hat{\boldsymbol{E}}^\top\hat{\boldsymbol{R}} = \boldsymbol{0}$. Moreover, it can be verified from (15) that

$$\begin{bmatrix} \operatorname{sym}(\bar{\boldsymbol{M}}_1\bar{\boldsymbol{A}}_{h\mu}) & \boldsymbol{E}^\top\bar{\boldsymbol{P}} + \bar{\boldsymbol{N}}\bar{\boldsymbol{R}}^\top - \bar{\boldsymbol{M}}_1 + (\bar{\boldsymbol{M}}_2\bar{\boldsymbol{A}}_{h\mu})^\top \\ * & -\operatorname{sym}(\bar{\boldsymbol{M}}_2) \end{bmatrix} < 0. \tag{18}$$

By performing the congruence transformation to (18) by $\begin{bmatrix}\boldsymbol{I}, \bar{\boldsymbol{A}}_{h\mu}^\top\end{bmatrix}$, we calculate

$$sym\Big(\bar{\boldsymbol{E}}^\top(\boldsymbol{P}\bar{\boldsymbol{A}}_{h\mu} - \bar{\boldsymbol{M}}_1^\top\bar{\boldsymbol{A}}_{h\mu} - \bar{\boldsymbol{M}}_2^\top\bar{\boldsymbol{A}}_{h\mu}) + \bar{\boldsymbol{N}}\bar{\boldsymbol{R}}^\top\bar{\boldsymbol{A}}_{h\mu}\Big) < 0. \tag{19}$$

Pre- and post-multiplying (19) by $\hat{\boldsymbol{W}}^\top$ and $\hat{\boldsymbol{W}}$, respectively, we obtain $\operatorname{sym}(\hat{\boldsymbol{N}}_{21}\hat{\boldsymbol{R}}_{21}^\top\hat{\boldsymbol{A}}_{22}) < 0$, according to (17). It may be inferred that $\bar{\boldsymbol{A}}_{h\mu}$ is non-singular and, based on the definition in [5], it is recognized that $(\bar{\boldsymbol{E}}, \bar{\boldsymbol{A}}_{h\mu})$ is both regular and impulse-free.

Let $\boldsymbol{\xi}(t) = \operatorname{col}\Big\{\bar{\boldsymbol{x}}(t),\ \bar{\boldsymbol{E}}\dot{\boldsymbol{x}}(t),\ \boldsymbol{\delta_s}(t)\Big\}$. To show the stability of closed-loop system (13), the subsequent Lyapunov function is selected as:

$$V(t) = \bar{\boldsymbol{x}}^\top(t)\bar{\boldsymbol{E}}^\top\bar{\boldsymbol{P}}\bar{\boldsymbol{E}}\bar{\boldsymbol{x}}(t). \tag{20}$$

Next, along the trajectories of system (13), we compute

$$\mathscr{L}\Big\{\dot{V}(t)\Big\} = 2\bar{\boldsymbol{x}}^\top(t)\bar{\boldsymbol{E}}^\top\bar{\boldsymbol{P}}\bar{\boldsymbol{E}}\dot{\bar{\boldsymbol{x}}}(t), \tag{21}$$

where $\mathscr{L}$ is the infinitesimal operator. As well, with the condition that $\bar{\boldsymbol{R}}^\top\bar{\boldsymbol{E}} = 0$, the following equations are valid for suitable matrices $\bar{\boldsymbol{N}}$ and $\bar{\boldsymbol{M}} = \operatorname{col}\Big\{\bar{\boldsymbol{M}}_1,\ \bar{\boldsymbol{M}}_2,\ \boldsymbol{0}\Big\}$:

$$2\bar{\boldsymbol{x}}^\top(t)\bar{\boldsymbol{N}}\bar{\boldsymbol{R}}^\top\bar{\boldsymbol{E}}\dot{\bar{\boldsymbol{x}}}(t) = \boldsymbol{0}, \tag{22}$$

and

$$\begin{aligned}\boldsymbol{0} =& \mathscr{L}\Big\{2\boldsymbol{\xi}^\top(t)\bar{\boldsymbol{M}}\Big(\bar{\boldsymbol{A}}_{h\mu}\bar{\boldsymbol{x}}(t) - \bar{\boldsymbol{E}}\dot{\bar{\boldsymbol{x}}}(t) + \bar{\zeta}\bar{\boldsymbol{L}}_\mu\boldsymbol{\delta}_s(t) + \bar{\boldsymbol{B}}_2\boldsymbol{g}_h(t) \\ &+ (\zeta(t) - \bar{\zeta})\bar{\boldsymbol{L}}_\mu\boldsymbol{\Gamma}(t)\Big)\Big\} \\ =& 2\boldsymbol{\xi}^\top(t)\bar{\boldsymbol{M}}\begin{bmatrix}\bar{\boldsymbol{A}}_{h\mu} & -\boldsymbol{I} & \bar{\zeta}\bar{\boldsymbol{L}}_\mu\end{bmatrix}\boldsymbol{\xi}(t) + 2\boldsymbol{\xi}^\top(t)\bar{\boldsymbol{M}}\bar{\boldsymbol{B}}_2\boldsymbol{g}_h(t).\end{aligned} \tag{23}$$

According to assumptions 1, it can be shown from Lemma 1

$$2\boldsymbol{\xi}^\top(t)\bar{\boldsymbol{M}}^\top\bar{\boldsymbol{B}}_2\boldsymbol{g}_h(t) \le \alpha^{-1}\boldsymbol{\xi}^\top(t)\bar{\boldsymbol{M}}\bar{\boldsymbol{B}}_2\hat{\boldsymbol{B}}_2^\top\bar{\boldsymbol{M}}^\top\boldsymbol{\xi}(t) + \alpha\delta^2\bar{\boldsymbol{x}}^\top(t)\hat{\boldsymbol{C}}_2^\top\hat{\boldsymbol{C}}_2\bar{\boldsymbol{x}}(t), \tag{24}$$

Moreover, it can be also established

$$-\tau\boldsymbol{\delta}_s^\top(t)\boldsymbol{\delta}_s(t) + \beta^2\tau\bar{\boldsymbol{x}}^\top(t)\hat{\boldsymbol{C}}_2^\top\hat{\boldsymbol{C}}_2\bar{\boldsymbol{x}}(t) \ge 0, \tag{25}$$

where τ is a positive scalar.

By adding (21)-(23) and considering conditions (24)-(25), we get

$$\mathscr{L}\Big\{\dot{V}(t)\Big\} \le \boldsymbol{\xi}^\top(t)\Big(\tilde{\boldsymbol{\Phi}}_{h\mu} + \alpha^{-1}\bar{\boldsymbol{M}}\bar{\boldsymbol{B}}_2\bar{\boldsymbol{B}}_2^\top\bar{\boldsymbol{M}}^\top\Big)\boldsymbol{\xi}(t), \tag{26}$$

where

$$\tilde{\boldsymbol{\Phi}}_{h\mu} = \begin{bmatrix} \boldsymbol{\Phi}_{11h\mu} & \boldsymbol{\Phi}_{12h\mu} & \bar{\zeta}\bar{\boldsymbol{M}}_1\bar{\boldsymbol{L}}_\mu \\ * & -\operatorname{sym}(\bar{\boldsymbol{M}}_2) & \bar{\zeta}\bar{\boldsymbol{M}}_2\bar{\boldsymbol{L}}_\mu \\ * & * & -\tau\boldsymbol{I} \end{bmatrix}. \tag{27}$$

Performing the Schur complement to (15), it easy to verify that

$$\hat{\boldsymbol{\Phi}}_{h\mu} = \tilde{\boldsymbol{\Phi}}_{h\mu} + \alpha^{-1}\bar{\boldsymbol{M}}\bar{\boldsymbol{B}}_2\bar{\boldsymbol{B}}_2^\top\bar{\boldsymbol{M}}^\top < 0, \tag{28}$$

Accordingly, we justify from (26) that

$$\mathscr{L}\Big\{\dot{V}(t)\Big\} \le \boldsymbol{\xi}^\top(t)\Big(\sum_{i=1}^{r}\sum_{j=1}^{r} h_i(\boldsymbol{x})\mu_j(\hat{\boldsymbol{x}})\hat{\boldsymbol{\Phi}}_{ij}\Big)\boldsymbol{\xi}(t) \le -\varsigma\|\boldsymbol{\xi}\|^2, \tag{29}$$

where

$\varsigma = \lambda_{min}(-\sum_{i=1}^{r}\sum_{j=1}^{r} h_i(\boldsymbol{x})\mu_j(\hat{\boldsymbol{x}})\hat{\boldsymbol{\Phi}}_{ij})$. Hence, it is evident the closed-loop system (13) is stochastically stable. ■

IV. Sliding Mode Dynamics Synthesis

This section outlines the methodology for synthesizing the gains $\boldsymbol{K}_i$ and $\boldsymbol{L}_i$ in Theorem 1. Before moving on, it is important to recall the following lemma.

Lemma 3. *[32] For given membership functions $h_i(\boldsymbol{x})$, $\mu_j(\hat{\boldsymbol{x}})$, and the constraint $\mu_j(\hat{\boldsymbol{x}}) - \varrho_j h_j(\hat{\boldsymbol{x}}) \ge 0,\ j \in \{1,\dots,r\}$ is satisfied for any positive scalar ϱ_i, if there exists a matrix $\boldsymbol{\Lambda}_i = \boldsymbol{\Lambda}_i^\top$ that satisfies $\boldsymbol{\Gamma}(\boldsymbol{\Pi}_{ij}, \boldsymbol{\Lambda}_i, \varrho_i) < \boldsymbol{0}$, where*

$$\boldsymbol{\Gamma}(\boldsymbol{\Pi}_{ij}, \boldsymbol{\Lambda}_i, \varrho_i) = \begin{cases} \boldsymbol{\Pi}_{ij} - \boldsymbol{\Lambda}_i < 0, \\ \varrho_i\boldsymbol{\Pi}_{ij} - \varrho_i\boldsymbol{\Lambda}_i + \boldsymbol{\Lambda}_i < 0, \\ \varrho_j\boldsymbol{\Pi}_{ij} + \varrho_i\boldsymbol{\Pi}_{ji} - \varrho_j\boldsymbol{\Lambda}_i - \varrho_i\boldsymbol{\Lambda}_j \\ +\boldsymbol{\Lambda}_i + \boldsymbol{\Lambda}_j < 0 \quad j > i, \end{cases} \tag{30}$$

then, $\sum_{i=1}^{r}\sum_{j=1}^{r} h_i(\boldsymbol{x})\mu_j(\hat{\boldsymbol{x}})\boldsymbol{\Pi}_{ij} < 0$ is fulfilled. In what follows, $\boldsymbol{\Gamma}(\boldsymbol{\Pi}_{ij}, \boldsymbol{\Lambda}_i, \varrho_i) < 0$, means that the conditions in (30) are satisfied.

Theorem 2. *For given positive scalars β, δ, and $\bar{\zeta}$, closed-loop system (13) is admissible, if for a set of positive scalars τ, α, $\lambda_q, q = 1,2,3,4$, ϱ_i, $i = 1,2,\cdots r$, and matrices $\bar{\boldsymbol{P}} > \boldsymbol{0}$, $\tilde{\boldsymbol{S}}$, $\bar{\boldsymbol{M}}_{11} \in \mathbb{R}^{n\times n}$, $\bar{\boldsymbol{M}}_{22} \in \mathbb{R}^{n\times n}$, $\bar{\boldsymbol{X}} \in \mathbb{R}^{m\times m}$, $\boldsymbol{Y}_j \in \mathbb{R}^{m\times n}$, $\boldsymbol{F}_j \in \mathbb{R}^{n\times n_y}$, the subsequent conditions are fulfilled according to the constraint $\mu_j(\hat{\boldsymbol{x}}) - \varrho_j h_j(\hat{\boldsymbol{x}}) \ge 0$.*

$$\boldsymbol{\Gamma}(\hat{\boldsymbol{\Pi}}_{ij}, \boldsymbol{\Lambda}_i, \varrho_i) < \boldsymbol{0}, \tag{31}$$

where

$\hat{\boldsymbol{\Pi}}_{ij} = \begin{bmatrix} \hat{\boldsymbol{\Pi}}_{ij}^1 & \hat{\boldsymbol{\Pi}}_{ij}^2 & \hat{\boldsymbol{\Pi}}_{ij}^3 \\ * & -\lambda_3\operatorname{sym}(\bar{\boldsymbol{X}}) & \boldsymbol{0} \\ * & * & -\lambda_4\operatorname{sym}(\bar{\boldsymbol{M}}_{22}) \end{bmatrix}$, $\hat{\boldsymbol{\Pi}}_{ij}^1 = \begin{bmatrix} \hat{\boldsymbol{\Pi}}_{ij}^{11} & \hat{\boldsymbol{\Pi}}_{ij}^{12} & \lambda_1\bar{\zeta}\mathbb{F}_j & \lambda_1\bar{\boldsymbol{M}}\bar{\boldsymbol{B}}_2 \\ * & \hat{\boldsymbol{\Pi}}_{ij}^{22} & \lambda_2\bar{\zeta}\mathbb{F}_j & \lambda_2\bar{\boldsymbol{M}}\bar{\boldsymbol{B}}_2 \\ * & * & -\tau\boldsymbol{I} & \boldsymbol{0} \\ * & * & * & -\alpha\boldsymbol{I} \end{bmatrix}$,

$\hat{\boldsymbol{\Pi}}_{ij}^2 = \begin{bmatrix}\lambda_1\boldsymbol{\Gamma}_1^{2\top} + \lambda_3\boldsymbol{\Gamma}_2^2 & \lambda_2\boldsymbol{\Gamma}_1^{2\top} & \boldsymbol{0} & \boldsymbol{0}\end{bmatrix}^\top$, $\hat{\boldsymbol{\Pi}}_{ij}^3 = \begin{bmatrix}\lambda_1\boldsymbol{\Gamma}_1^{3\top} + \lambda_4\boldsymbol{\Gamma}_2^3 & \lambda_2\boldsymbol{\Gamma}_1^{3\top} & -\lambda_4\boldsymbol{F}^\top & \boldsymbol{0}\end{bmatrix}^\top$,

$\boldsymbol{\Gamma}_1^2 = \bar{\boldsymbol{M}}\bar{\boldsymbol{B}}_2 - \bar{\boldsymbol{B}}_2\bar{\boldsymbol{X}}$, $\boldsymbol{\Gamma}_2^2 = \begin{bmatrix}\boldsymbol{Y}_j & \boldsymbol{0}\end{bmatrix}$ $\boldsymbol{\Gamma}_1^3 = \begin{bmatrix}\bar{\boldsymbol{M}}_{11}\tilde{\boldsymbol{S}} - \bar{\boldsymbol{M}}_{22} \\ \boldsymbol{0}\end{bmatrix}$, $\boldsymbol{\Gamma}_2^3 = \begin{bmatrix}\bar{\zeta}\boldsymbol{F}_j\boldsymbol{C}_2 & -(1-\bar{\zeta})\boldsymbol{F}_j\boldsymbol{C}_2\end{bmatrix}$, $\hat{\boldsymbol{\Pi}}_{ij}^{11} = \lambda_1\operatorname{sym}(\mathbb{A}_{ij}) + (\tau\beta^2 + \alpha\delta^2)\hat{\boldsymbol{C}}_2^\top\hat{\boldsymbol{C}}_2$, $\hat{\boldsymbol{\Pi}}_{ij}^{12} = (\bar{\boldsymbol{P}}\bar{\boldsymbol{E}} + \bar{\boldsymbol{N}}\bar{\boldsymbol{R}})^\top - \lambda_1\bar{\boldsymbol{M}} + \lambda_2\mathbb{A}_{ij}$, $\hat{\boldsymbol{\Pi}}_{ij}^{22} = -\lambda_2\operatorname{sym}(\bar{\boldsymbol{M}})$,

$\mathbb{A}_{ij} = \begin{bmatrix}\bar{\boldsymbol{M}}_{11}\boldsymbol{A}_j + \boldsymbol{B}_2\boldsymbol{Y}_j + \bar{\zeta}\tilde{\boldsymbol{S}}\boldsymbol{F}_j\boldsymbol{C}_2 & \bar{\boldsymbol{M}}_{11}\boldsymbol{A}_j + (1-\bar{\zeta})\tilde{\boldsymbol{S}}\boldsymbol{F}_j\boldsymbol{C}_2 \\ \bar{\boldsymbol{M}}_{22}(\boldsymbol{A}_i - \boldsymbol{A}_j) + \bar{\zeta}\boldsymbol{F}_j\boldsymbol{C}_2 & \bar{\boldsymbol{M}}_{22}\boldsymbol{A}_i - (1-\bar{\zeta})\boldsymbol{F}_j\boldsymbol{C}_2\end{bmatrix}$, $\bar{\boldsymbol{M}} = \begin{bmatrix}\bar{\boldsymbol{M}}_{11} & \bar{\boldsymbol{M}}_{11} \\ \boldsymbol{0} & \bar{\boldsymbol{M}}_{22}\end{bmatrix}$ $\mathbb{F}_j = \begin{bmatrix}-\boldsymbol{F}_j \\ -\boldsymbol{F}_j\end{bmatrix}$, $\bar{\boldsymbol{B}}_2 = \begin{bmatrix}\boldsymbol{B}_2 \\ \boldsymbol{0}\end{bmatrix}$.

Moreover, the parameters $\boldsymbol{K}_j$ and $\boldsymbol{L}_j$ are given by $\boldsymbol{K}_j = \bar{\boldsymbol{X}}^{-1}\boldsymbol{Y}_j$ and $\boldsymbol{L}_j = (\bar{\boldsymbol{M}}_{22})^{-1}\boldsymbol{F}_j$, respectively.

Proof: If the conditions in Theorem 2 are true, the constraints $-\lambda_4\operatorname{sym}(\bar{\boldsymbol{M}}_{22}) < 0$ and $-\lambda_3\operatorname{sym}(\bar{\boldsymbol{X}}) < 0$ are also true, and matrices $\bar{\boldsymbol{M}}_{22}$, and $\bar{\boldsymbol{X}}$ are non-singular.

According to Lemma 3, we obtain

$$\sum_{i=1}^{r}\sum_{j=1}^{r} h_i(\boldsymbol{x})\mu_j(\hat{\boldsymbol{x}})\hat{\boldsymbol{\Pi}}_{ij} < 0. \tag{32}$$

Note that $\bar{\boldsymbol{M}}\bar{\boldsymbol{A}}_{ij} = \mathbb{A}_{ij} + \boldsymbol{\Gamma}_1^2\bar{\boldsymbol{X}}^{-1}\boldsymbol{\Gamma}_2^2 + \boldsymbol{\Gamma}_1^3\bar{\boldsymbol{M}}_{22}^{-1}\boldsymbol{\Gamma}_2^3$, and $\bar{\boldsymbol{M}}\bar{\boldsymbol{L}}_j = \mathbb{F}_j - \boldsymbol{\Gamma}_1^3\bar{\boldsymbol{M}}_{22}^{-1}\boldsymbol{F}_j$.

Then, based on Lemma 2, it can be demonstrated that $\sum_{i=1}^{r}\sum_{j=1}^{r} h_i(\boldsymbol{x})\mu_j(\hat{\boldsymbol{x}})\hat{\boldsymbol{\Pi}}_{ij}^1 < \boldsymbol{0}$. Referring to the Schur complement, the condition in Eq. (15) is satisfied. This implies that system (13) is stochastically admissible. ■

A. Adaptive Sliding Mode Controller Design

This section is devoted to synthesize an adaptive sliding mode controller to achieve the reachability of the sliding surface described by Eq. (9). Simultaneously, the system's trajectory described by Eq. (7) may be directed onto the sliding surface and stay on it thereafter. To begin, we will use the RBF neural network, which has the benefit of a simple structure and fast convergence, to estimate the term $\boldsymbol{\delta}_g(t) = \boldsymbol{\delta}_a(t) + \boldsymbol{g}_h(t)$. According to the reference [36], [37], there exists a radial basis function neural network (RBFNN) able to approximate the unknown function $\boldsymbol{\delta}_g(t)$ over a compact set Ω that can be expressed as follows:

$$\boldsymbol{\delta}_g(t) = \boldsymbol{W}^{*\top}\boldsymbol{\psi}(\hat{\boldsymbol{x}}(t)) + \varepsilon(t),$$

where $\boldsymbol{W}^*$ represents the optimal weight satisfying $\boldsymbol{W}^* = \arg\min_{\boldsymbol{W}}(\sup_\Omega \|\boldsymbol{\delta}_g(t) - \hat{\boldsymbol{\delta}}_g(t)\|)$, and $\varepsilon(t)$ stands for the approximation error so that for $\epsilon > 0$, $\|\varepsilon(t)\| \le \epsilon$. The estimated function $\hat{\boldsymbol{\delta}}_g(t)$ is defined as $\hat{\boldsymbol{\delta}}_g(t) = \hat{\boldsymbol{W}}^\top\boldsymbol{\psi}(\hat{\boldsymbol{x}}(t))$, where

$\hat{\boldsymbol{W}} = [\hat{\boldsymbol{W}}_1,\ \hat{\boldsymbol{W}}_2, \cdots, \hat{\boldsymbol{W}}_m]$ defines for the matrix of the neural-network weights so that $\hat{\boldsymbol{W}}_k^\top = [\hat{\boldsymbol{w}}_k^1,\ \hat{\boldsymbol{w}}_k^2, \cdots, \hat{\boldsymbol{w}}_k^N]$, $k = 1, 2, \cdots, m$, and N represents the number of hidden nodes. $\boldsymbol{\psi}(\hat{\boldsymbol{x}}) = [\psi_1(\hat{\boldsymbol{x}}),\ \psi_2(\hat{\boldsymbol{x}}),\ ,\cdots \psi_N(\hat{\boldsymbol{x}})]^\top$ specifies the regression functions vector, where the Gaussian RBF $\psi_k(\hat{\boldsymbol{x}})$ is expressed as $\psi_k(\hat{\boldsymbol{x}}) = \exp\Big(-\dfrac{\|\hat{\boldsymbol{x}} - c_k\|^2}{{d_k}^2}\Big)$, where c_k is the centre and $d_k > 0$ is the width of the Gaussian. On the other hand , due to the sensor attack, a precise calculation of the term $\bar{\boldsymbol{S}}\boldsymbol{L}_\mu(\tilde{\boldsymbol{y}}(t) - \hat{\boldsymbol{y}}(t))$ becomes difficult. That is why it may be inferred that there exist some scalars so that $\|\bar{\boldsymbol{S}}\boldsymbol{L}_\mu\|\|(\tilde{\boldsymbol{y}}(t) - \hat{\boldsymbol{y}}(t))\| \le \rho_1\|\boldsymbol{y}(t)\| + \rho_2\|\hat{\boldsymbol{y}}(t)\|$, where the unknown scalars $\rho_l, l = 1, 2$ should be estimated.

Theorem 3. *Suppose that sliding function Eq.* (9) *is appropriately designed and the gains* $\boldsymbol{K}_i$ *and* $\boldsymbol{L}_i$ *are solved in Theorem 2. Under the control in Eq.* (33)*, the trajectories of Eq.* (7) *can be driven to sliding surface* $\boldsymbol{s}(t) = 0$ *and maintain the sliding motion thereafter.*

$$\begin{aligned}\boldsymbol{u}(t) = &\sum_{j=1}^{r} \mu_j(\boldsymbol{\varphi}(\hat{\boldsymbol{x}}))\Big(\boldsymbol{K}_j\hat{\boldsymbol{x}}(t) - (\bar{\boldsymbol{S}}\boldsymbol{B}_2)^{-1}\Big(\hat{\boldsymbol{W}}^\top\boldsymbol{\psi}(\hat{\boldsymbol{x}}(t)) \\ &+ (\hat{\rho}_1(t)\|\boldsymbol{y}(t)\| + \hat{\rho}_2(t)\|\hat{\boldsymbol{y}}(t)\| + \hat{\epsilon}(t) + \kappa)\frac{\boldsymbol{s}(t)}{\|\boldsymbol{s}(t)\|}\Big)\Big),\end{aligned} \tag{33}$$

where $\kappa > 0$ *is a small constant, and for positive constants* $q_l,\ l = 0, 1, \cdots, 3$*, the adaptive parameters are characterized by*

$$\dot{\hat{W}}_k = q_0 s_k \boldsymbol{\psi}(\hat{\boldsymbol{x}}(t)),\ \dot{\hat{\rho}}_1(t) = q_1\|\boldsymbol{y}(t)\|\|\boldsymbol{s}(t)\|, \tag{34}$$

$$\dot{\hat{\rho}}_2(t) = q_2\|\hat{\boldsymbol{y}}(t)\|\|\boldsymbol{s}(t)\|,\ \dot{\hat{\epsilon}}(t) = q_3\|\boldsymbol{s}(t)\|. \tag{35}$$

Proof: Construct a Lyapunov function defined as follows:

$$\begin{aligned}V_s(t) = &\frac{1}{2}\boldsymbol{s}^\top(t)\boldsymbol{s}(t) + \frac{1}{2q_0}\sum_{k=1}^{m}\tilde{\boldsymbol{W}}_k^\top\tilde{\boldsymbol{W}}_k + \frac{1}{2q_1}\tilde{\rho}_1^2(t) \\ &+ \frac{1}{2q_2}\tilde{\rho}_2^2(t) + \frac{1}{2q_3}\tilde{\epsilon}^2(t),\end{aligned} \tag{36}$$

where $\tilde{\boldsymbol{W}}_k = \hat{\boldsymbol{W}}_k - \boldsymbol{W}_k^*$, $\tilde{\rho}_1(t) = \rho_1 - \hat{\rho}_1(t)$, $\tilde{\rho}_2(t) = \rho_2 - \hat{\rho}_2(t)$, and $\tilde{\epsilon}(t) = \epsilon - \hat{\epsilon}(t)$.

The derivative computation of $\boldsymbol{s}(t)$ and $V_s(t)$ leads, respectively, to

$$\begin{aligned}\dot{V}_s(t) =&\boldsymbol{s}^\top(t)\dot{\boldsymbol{s}}(t) + \frac{1}{q_0}\sum_{k=1}^{m}\tilde{\boldsymbol{W}}_k^\top\dot{\tilde{\boldsymbol{W}}}_k + \frac{1}{q_1}\tilde{\rho}_1(t)\dot{\tilde{\rho}}_1(t) \\ &+ \frac{1}{q_2}\tilde{\rho}_2(t)\dot{\tilde{\rho}}_2(t) + \frac{1}{q_3}\tilde{\epsilon}(t)\dot{\tilde{\epsilon}}(t), \\ =&\boldsymbol{s}^\top(t)\Big(\bar{\boldsymbol{S}}\boldsymbol{B}_2(\boldsymbol{u}(t) + \boldsymbol{\delta}_g(t) - \boldsymbol{K}_j\hat{\boldsymbol{x}}(t)) \\ &+ \bar{\boldsymbol{S}}\boldsymbol{L}_\mu(\tilde{\boldsymbol{y}}(t) - \hat{\boldsymbol{y}}(t))\Big) + \frac{1}{q_0}\sum_{k=1}^{m}\tilde{\boldsymbol{W}}_k^\top\dot{\tilde{\boldsymbol{W}}}_k \\ &+ \frac{1}{q_1}\tilde{\rho}_1(t)\dot{\tilde{\rho}}_1(t) + \frac{1}{q_2}\tilde{\rho}_2(t)\dot{\tilde{\rho}}_2(t) + \frac{1}{q_3}\tilde{\epsilon}(t)\dot{\tilde{\epsilon}}(t), \\ \le&\boldsymbol{s}^\top(t)\Big(\tilde{\boldsymbol{W}}^\top\boldsymbol{\psi}(\hat{\boldsymbol{x}}(t)) + \tilde{\epsilon}(t) + (\tilde{\rho}_1(t)\|\boldsymbol{y}(t)\| + \\ &\tilde{\rho}_2(t)\|\hat{\boldsymbol{y}}(t)\| + \kappa)\frac{\boldsymbol{s}(t)}{\|\boldsymbol{s}(t)\|}\Big) + \frac{1}{q_0}\sum_{k=1}^{m}\tilde{\boldsymbol{W}}_k^\top\dot{\tilde{\boldsymbol{W}}}_k \\ &+ \frac{1}{q_1}\tilde{\rho}_1(t)\dot{\tilde{\rho}}_1(t) + \frac{1}{q_2}\tilde{\rho}_2(t)\dot{\tilde{\rho}}_2(t) + \frac{1}{q_3}\tilde{\epsilon}(t)\dot{\tilde{\epsilon}}(t).\end{aligned} \tag{37}$$

Considering the update laws (34) and using the fact that $\dot{\tilde{\boldsymbol{W}}}_k = -\dot{\hat{\boldsymbol{W}}}_k$, $\dot{\tilde{\rho}}_1(t) = -\dot{\hat{\rho}}_1(t)$, $\dot{\tilde{\rho}}_2(t) = -\dot{\hat{\rho}}_2(t)$, and $\dot{\tilde{\epsilon}}(t) = -\dot{\hat{\epsilon}}(t)$ it can be computed

$$\begin{aligned}&\frac{1}{q_0}\sum_{k=1}^{m}\tilde{\boldsymbol{W}}_k^\top\dot{\tilde{\boldsymbol{W}}}_k + \frac{1}{q_1}\tilde{\rho}_1(t)\dot{\tilde{\rho}}_1(t) + \frac{1}{q_2}\tilde{\rho}_1(t)\dot{\tilde{\rho}}_2(t) + \frac{1}{q_3}\tilde{\epsilon}(t)\dot{\tilde{\epsilon}}(t) \\ &= -\boldsymbol{s}^\top(t)\tilde{\boldsymbol{W}}^\top\boldsymbol{\psi}(\hat{\boldsymbol{x}}(t)) \\ &- (\tilde{\rho}_1(t)\|\boldsymbol{y}(t)\| + \tilde{\rho}_2(t)\|\hat{\boldsymbol{y}}(t)\| + \tilde{\epsilon}(t))\|\boldsymbol{s}(t)\|.\end{aligned} \tag{38}$$

Substituting (38) into (37) one gets

$$\dot{V}_s(t) \le -\kappa\|\boldsymbol{s}(t)\|. \tag{39}$$

which confirms that the adaptive control law Eq. (33) is capable of driving the system dynamics onto the sliding surface Eq. (9) despite the presence of attacks.

■

V. SMC Design and Optimization

A. Problem Statement

It is obvious from theorems 1-2 that the significant challenge in developing the SMC law Eq. (33) lies in determining the appropriate sliding matrix $\bar{\boldsymbol{S}}$ that meets the constraint condition $\det(\bar{\boldsymbol{S}}\boldsymbol{B}_2) \neq 0$, along with the controller and observer gain matrices $\boldsymbol{K}_j$ and $\boldsymbol{L}_j$ satisfy the conditions in Eq. (31). Moreover, it is clear that the tuning parameters λ_q in Eq. (31) are not easily obtainable, making it a difficult task. Furthermore, inappropriate gains $\boldsymbol{K}_j$ and $\boldsymbol{L}_j$ might amplify the impact of attacks on degrading the system's performance.

B. Optimization Problem

As previously mentioned, the sliding matrix $\bar{\boldsymbol{S}}$ plays a crucial role in the SMC design, influencing the dynamic performance of the controlled system. In addition, reducing the values of $\boldsymbol{K}_i$ and $\boldsymbol{L}_i$ leads to decreased amplification of the attack's signals, potentially reducing the impact of any attacks. Thus, it is logical to search an appropriate sliding matrix $\bar{\boldsymbol{S}}$ able to provide the optimized gain $\boldsymbol{K}_i$ and $\boldsymbol{L}_i$. To figure out how to achieve this goal, we formulate the following optimization problem:

$$\begin{aligned}&\min \Omega = \sum_{i=1}^{r}\Big(\gamma\|\boldsymbol{K}_i\| + (1-\gamma)\|\boldsymbol{L}_i\|\Big), \\ &\text{subject to} \qquad (31)\end{aligned} \tag{40}$$

where the weighting parameter $\gamma \in [0,\ 1]$.

To deal with the problem as expressed in Eq. (40) many evolutionary techniques, such as the genetic algorithm [25], the PSO algorithm [26], and the dandelion [28], [29] can be used. These techniques have proven to be highly effective in addressing nonlinear and non-convex optimization problems with constraints. Hence, we explore the combination of the optimization algorithm SBOA [39] and LMI techniques to tackle the sliding mode control design by solving the previously mentioned problem.

Remark 2. The secretary bird optimization algorithm (SBOA) has been recently introduced in [39] as a new meta-heuristic algorithm. This algorithm is specifically established by observing the hunting and evading abilities of secretary birds while dealing with predators. The two primary phases of this algorithm that simulate the behavior of secretary birds in collecting snakes and escaping predators are, respectively, the exploration and the exploitation. The reliability of the algorithm is tested in [39] through several engineering optimization design problems.

To carry out the SBOA algorithm, we express in the search space the secretary birds positions as a row vector ϖ defined as $[\bar{\boldsymbol{S}}, \lambda_1, \ldots \lambda_4] \longrightarrow \varpi = [s_{11}, \ldots, s_{1n}, s_{21} \ldots, s_{mn}, \lambda_1, \ldots \lambda_4]$.

Assume that, each element s_{mn} has a range of $s_{mn} \in [\underline{s}_{mn},\ \bar{s}_{mn}]$, and $\lambda_l \in [\underline{\lambda}_l,\ \bar{\lambda}_l]$, where $\underline{\lambda}_l > 0,\ \bar{\lambda}_l > 0$.

Algorithm 1, and the flowchart depicted in Fig. 2, describe the different steps of the optimal SMC design using the SBOA as detailed in [39]. Algorithm 1 will be performed 30 times to achieve the optimal gains $\boldsymbol{K}_i$, $\boldsymbol{L}_i$, sliding matrix $\bar{\boldsymbol{S}}$, and parameters λ_q.

Algorithm 1 SBOA Algorithm for SMC Law Design

- **Input**: The population size, denoted as N, the dimension of the variables, denoted as n_d, and the maximum number of iterations, denoted as $Niter$.
- **Output**: The optimal individual, denoted as ϖ_{best}, and the corresponding fitness value, denoted as Ω_{best}.

1) **Step 1**: **Encoding phase**.
Each element of the row vector $\varpi = [s_{11}, \ldots, s_{1n}, s_{21} \ldots, s_{mn}, \lambda_1, \ldots \lambda_4]$ can be encoded as a bird.
2) **Step 2**: **Population initialization**.
Generate an initial population of N individuals $\varpi_v,\ (v = 1, 2, \ldots, N)$ at random.
3) **Step 3**: **Fitness function and assignment**: Calculation of the fitness for the individual by solving the LMIs (31).
4) **Step 4 Reproduction Phase:** According to the obtained fitness values in previous step, the **exploration** and **exploitation** operations should be performed as crucial steps of the SBOA.
5) **Step 5**: **Design Phase**: Produce the SMC law (33) by using the sliding matrix $\bar{\boldsymbol{S}}$ and the gain matrices $\boldsymbol{K}_i$, and $\boldsymbol{L}_i$ obtained in step 4.

VI. Simulation Studies

This section employs a nonlinear system for disc rolling on a surface without sliding, as a means to showcase the feasibility and benefits of the proposed method. As mentioned in [38], the system under study may be described by the following mathematical model:

$$\begin{cases} \dot{x}_1 = x_2, \\ \dot{x}_2 = -(\dfrac{K_1}{m}x_1 + \dfrac{K_2}{m}x_1^3) - \dfrac{b}{m}x_2 + \dfrac{1}{m}x_4, \\ 0 = x_2 - r x_3, \\ 0 = -(\dfrac{K_1}{m}x_1 + \dfrac{K_2}{m}x_1^3) - \dfrac{b}{m}x_2 + (\dfrac{r^2}{J} + \dfrac{1}{m})x_4 - \dfrac{r}{J}u. \end{cases} \tag{41}$$

Moreover, the assumption $x_1(t) \in [-1,\ 1]$ allows us to explore the sector non-linearity approach for converting the non-linear system into the equivalent TS fuzzy descriptor model Eq. (2) with membership functions defined as $h_1(x_1(t)) = 1 - x_1^2(t)$, and $h_2(x_1(t)) = x_1^2(t)$. The relevant model data are given as $\boldsymbol{E} = \mathrm{diag}\{1, 1, 0, 0\}$, $\boldsymbol{A}_i = \begin{bmatrix} 0 & 1 & 0 & 0 \\ a\{i\} & -0.75 & 0 & 0.025 \\ 0 & 1 & -0.4 & 0 \\ b\{i\} & -0.75 & 0 & 0.075 \end{bmatrix}$, $\boldsymbol{B}_2 = \begin{bmatrix} 0 \\ 0 \\ 0 \\ -0.125 \end{bmatrix}$, $\boldsymbol{C}_2 = \begin{bmatrix} 1 & 0 & 0 & 0 \\ 0 & 1 & 0 & 0 \end{bmatrix}$ $a \in \{-2.5, -5\}$, $b \in \{-2.5, -5\}$, $i = 1, 2$.

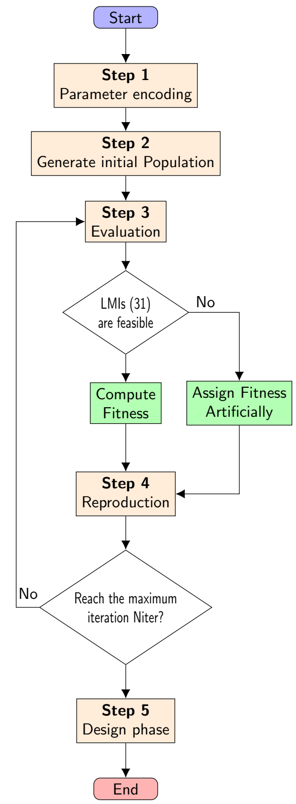

Fig. 2. Flowchart of the proposed SMC with SBOA and LMIs.

A. Simulation Studies and Discussions

Once the fuzzy model of the system has been introduced, we assess the resilience and robustness of the system by considering different scenarios. We begin with scenario I, which involves designing and implementing a controller that is not optimized, to thoroughly evaluate its resilience against different threats.

Case I Here we explore the strategy developed in Theorem 2, tailored to shield the system from sensor and actuator deception attacks. We leverage Yalmip, a MATLAB toolbox specifically developed for optimization modeling, and Mosek, an efficient and accurate solver well recognized for its ability to solve complex optimization problems on a large scale. By carefully selecting key design parameters, $\bar{\boldsymbol{S}} = [2 \quad 2 \quad -1 \quad -8]$, so that $\bar{\boldsymbol{S}}\boldsymbol{B}_2 = \boldsymbol{I}$, $\beta = 0.35$, $\delta = 0.2$, $\lambda_{1,2} = 1$, and $\lambda_{3,4} = 0.35$, we effectively derive the controller and observer gain matrices $\boldsymbol{K}_1 = \begin{bmatrix} 0.0269 & -0.0098 & 0.0053 & 0.2910 \end{bmatrix}$, $\boldsymbol{K}_2 = \begin{bmatrix} 0.0404 & -0.0091 & 0.0070 & 0.2973 \end{bmatrix}$, $\boldsymbol{L}_1 = \begin{bmatrix} 1.5592 & -0.5933 \\ -1.7422 & 8.4758 \\ 1.0001 & 0.9889 \\ -1.2624 & 6.9014 \end{bmatrix}$, $\boldsymbol{L}_2 = \begin{bmatrix} 1.8422 & -0.6246 \\ -2.1511 & 8.7691 \\ 1.3088 & 0.9851 \\ -1.7590 & 7.1692 \end{bmatrix}$.

To simulate realistic cyber-physical threats, we establish precise models for both sensor and actuator attacks. The sensor attack model, $\boldsymbol{\delta}_s(t)$, represents possible disturbances in sensor measurements and is defined as

$$\boldsymbol{\delta}_s(t) = \begin{cases} b, & t < 2, b \in [-0.5,\ 0.5], \\ 0.1\boldsymbol{y}(t) + 0.2\boldsymbol{y}(t)\sin(100t), & 2 \le t < 10, \\ bt\tanh(0.5\boldsymbol{y}(t)), & 10 \le t \le 25. \end{cases}$$

Moreover, we assign the probability of encountering sensor as $\bar{\zeta} = 0.3$, and we assume that the actuator attack model is expressed as $\boldsymbol{\delta}_a(t) = 0.3\tanh(-3x_2(t))$. Setting the initial conditions of the system and the observer as $\boldsymbol{x}(0) = \begin{bmatrix}0.25 & 0.6 & 0.4 & 1\end{bmatrix}^T$, and $\hat{\boldsymbol{x}}(0) = \begin{bmatrix}0 & 0 & 0 & 0\end{bmatrix}^T$, we perform 50 random independent simulations a simulation to robustly test the system's resilience against attacks in which the membership functions of the fuzzy controller are defined as $\mu_1(\hat{x}_1(t)) = \Big(1 - \dfrac{1}{1+e^{-20(\hat{x}_1(t)-\frac{\pi}{8})}}\Big)\Big(\dfrac{1}{1+e^{-20(\hat{x}_1(t)+\frac{\pi}{8})}}\Big)$, $\mu_2(\hat{x}_1(t)) = 1 - \mu_1(\hat{x}_1(t))$.

We assume that the matched external disturbance has the following form: $\boldsymbol{g}(t) = 0.1\sin(x_2(t))\cos(x_1(t)$.

Fig. 3(a)-(b) display the results of these simulations, notably highlighting the effectiveness of the closed-loop system with the implemented control strategy, as described in Eq. (9)-(33). The adaptive laws defined in Eq. (34) are used under zero initial conditions and the parameters are specified as $q_l = 0.35,\ l = 0,\cdots,3$. Furthermore, to reduce the occurrence of chattering in the control signal, we substitute the function $\boldsymbol{s}(t)/\|\boldsymbol{s}(t)\|$ with $\boldsymbol{s}(t)/(\|\boldsymbol{s}(t)+0.01\|)$. The results of these simulations demonstrate that although the system is resilient to attacks, the observer struggles to properly estimate the states x_3, and x_4. Now we will concentrate on Case II and employ the optimization problem in Eq. (40) to solve this issue.

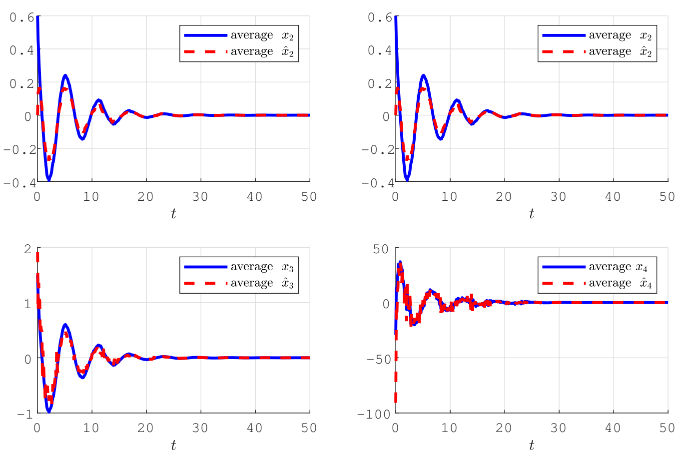

(a)

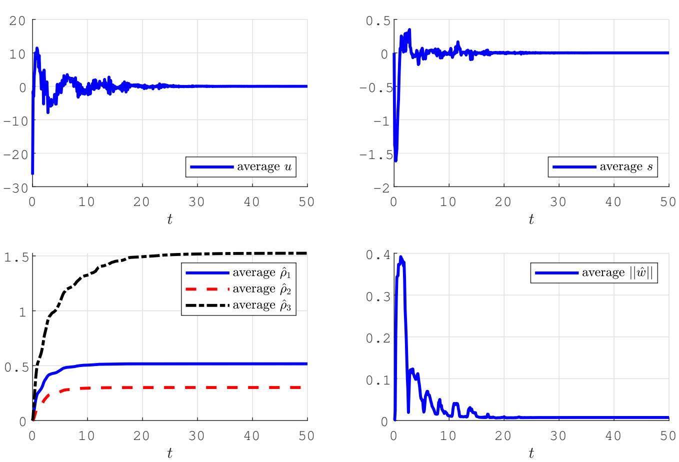

(b)

Fig. 3. Performance and closed-loop behavior with the implemented non-optimized control strategy.

Case II In this case, we explore the optimization problem Eq. (40) to improve the system's performance by reducing the observer and controller gains. By exploiting Algorithm 1, the outcomes of are found as $\bar{\boldsymbol{S}} = [2\ 1.5254\ -1\ -9.8984]$, $\lambda_1 = 0.73993$, $\lambda_2 = 1.7955$, $\lambda_3 = 1.6335$, $\lambda_4 = 1.9346$,
$\boldsymbol{K}_1 = \begin{bmatrix}0.001267 & -0.000329 & 0.000258 & 0.058563\end{bmatrix}$,
$\boldsymbol{K}_2 = \begin{bmatrix}-0.000381 & -0.000202 & -0.000347 & 0.058733\end{bmatrix}$, $\boldsymbol{L}_1 = \begin{bmatrix}0.85563 & 0.27457\\ -0.36813 & 2.1366\\ 0.6122 & 0.31301\\ -0.36818 & 1.6922\end{bmatrix}$, $\boldsymbol{L}_2 = \begin{bmatrix}0.86772 & 0.25946\\ -0.50868 & 2.239\\ 0.62446 & 0.2974\\ -0.47119 & 1.7995\end{bmatrix}$

The evolution of the best and average fitness values are shown in Fig. 4.

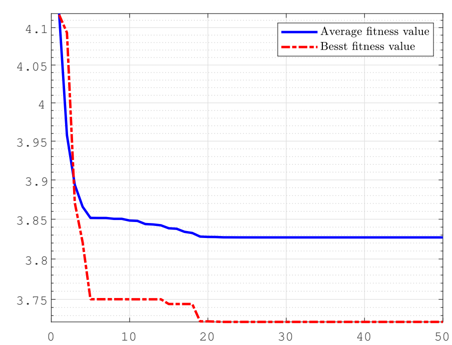

Fig. 4. Evolution of the fitness function in solving the optimization problem using SBOA.

Fig. 5(a)-(b) display the average results of simulations, focusing on the system and observer states with the applied control strategy under similar initial conditions and system parameters while employing the aforementioned gains. Besides, The sliding function in Eq. (9) and the estimation of unknown variables are also provided in sub-figure (b). These figures prove that, despite the presence of deception attacks targeting both sensors and actuators, the closed-loop states remain stable over time and the observer accurately estimate the unmeasured states. The findings from Case II show that, despite the complexity and high computational cost of Algorithm 1, it has the potential to design an optimized control law able to enhance the accuracy of the observer in cyber-physical systems.

Case III Here, we compare our suggested control technique with the control scheme presented in [34], [35] to emphasis the superiority of our method. Employing the following gains $\boldsymbol{K}_1 = \begin{bmatrix}-19.4666 & -5.3215 & 0.0416 & 3.8020\end{bmatrix}$, $\boldsymbol{K}_2 = \begin{bmatrix}-24.4577 & -5.2564 & 0.0419 & 3.8023\end{bmatrix}$,

$$\boldsymbol{L}_1 = \begin{bmatrix}7.2599 & 2.4086\\ -1.3326 & 5.2242\\ -0.1383 & 0.6004\\ -2.8994 & -1.0296\end{bmatrix}, \boldsymbol{L}_2 = \begin{bmatrix}7.2697 & 2.3827\\ -1.4514 & 5.4131\\ 0.0888 & 0.7158\\ -3.0922 & -0.8722\end{bmatrix}.$$

Fig. 6(a)-(b) demonstrate that implementing the SMC law [34], [35] under similar initial conditions and model parameters reduces significantly the system's effectiveness.

Fig. 7 depicts the estimation error for the previous cases by performing 50 random independent trials. Taken together, Cases I, II, and III, demonstrate that the proposed secure SMC control law can significantly improve the robustness and effectiveness of systems dealing with attacks. Moreover, we evaluate for each case the input energy as displayed in Table I. The table confirms that the optimized scenario uses the least amount of energy with the best control capabilities.

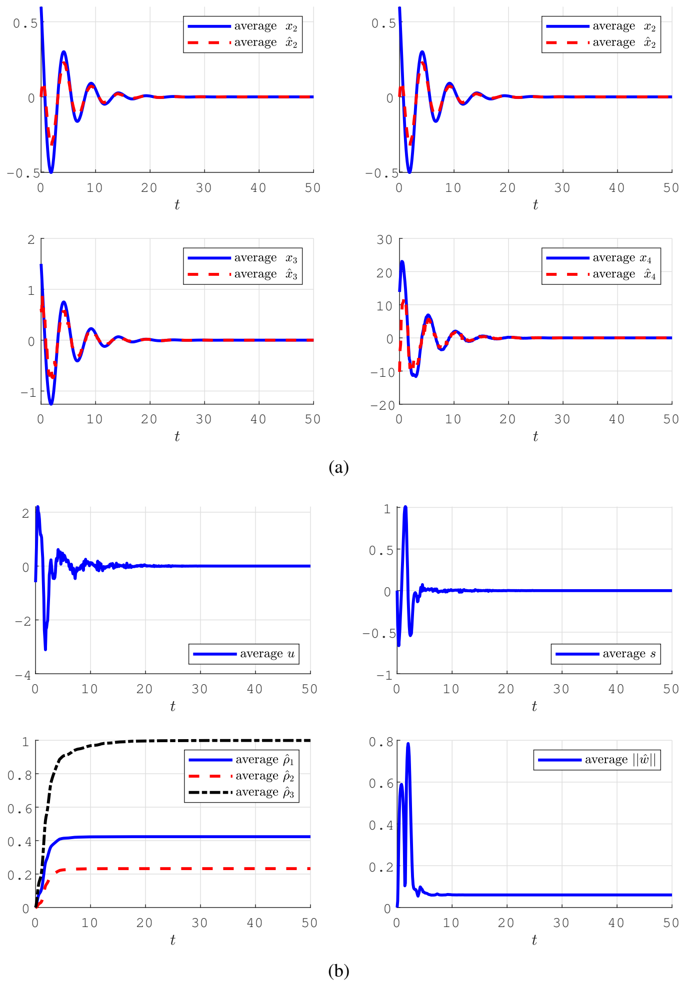

Fig. 5. Performance and behavior of the closed-loop system with the performed optimized control strategy.

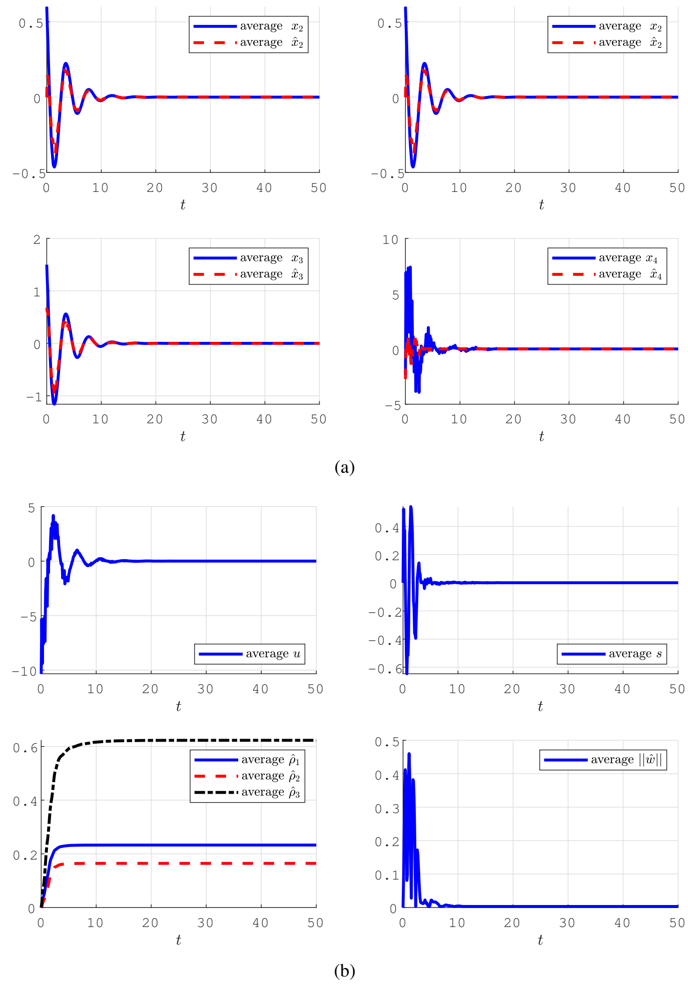

Fig. 6. Comparison of the closed-loop trajectories using the control scheme from [34], [35], highlighting differences in system performances.

TABLE I. INPUT ENERGY FOR EACH CASE

Input Energy	Case I	Case II	Case III
$\|\boldsymbol{u}(t)\|$	11.3016	48.8997	26.1262

VII. CONCLUSIONS AND FUTURE WORK

This work investigated an advanced control scheme that integrates the SMC methodology in conjunction with a meta-heuristic method in order to address the challenge of security control for nonlinear systems that are susceptible to deception attacks on their sensors and actuators. This scheme is based on developing an observer-based sliding mode control law for nonlinear descriptor systems described by TS fuzzy models. The admissibility and reachability features are established by satisfactory sufficient conditions, and the SBOA is investigated to tackle an optimization problem with non-convex and nonlinear constraints in order to enhance the system's performance under threats. An extensive analysis of a practical example divided into multiple cases revealed that the proposed method significantly improved system resilience and efficiency in the face of diverse cyber-attacks. This analysis especially highlighted the method's superiority over previous strategies proposed in [34], [35].

Several promising research directions arise from this work. A key priority for future investigation is the effect of network-induced delays and actuator/sensor saturation constraints on the performance of cyber-secure control systems, as these real-world limitations can be exploited by advanced attackers. Further exploration is also needed to extend the proposed framework to distributed control architectures for multi-agent systems, incorporate machine learning-based adaptive security mechanisms with event-triggered protocols.

ACKNOWLEDGMENTS

This Project was funded by the Deanship of Scientific Research (DSR) at King Abdulaziz University, Jeddah, under grant no.(GPIP: 1234-135-2024). The authors, therefore, acknowledge with thanks DSR for technical and financial support.

REFERENCES

[1] Z.-G. Wu, S. Dong, P. Shi, D. Zhang, T. Huang, Reliable filter design of takagi–sugeno fuzzy switched systems with imprecise modes, IEEE Transactions on Cybernetics 50 (5) (2020) 1941–1951.

[2] Y. Wang, C. K. Ahn, H. Yan, S. Xie, Fuzzy control and filtering for nonlinear singularly perturbed markov jump systems, IEEE Transactions on Cybernetics 51 (1) (2021) 297–308.

[3] N. Zhang, W. Qi, G. Pang, J. Cheng, K. Shi, Observer-based sliding mode control for fuzzy stochastic switching systems with deception attacks, Applied Mathematics and Computation, 427, (2022)

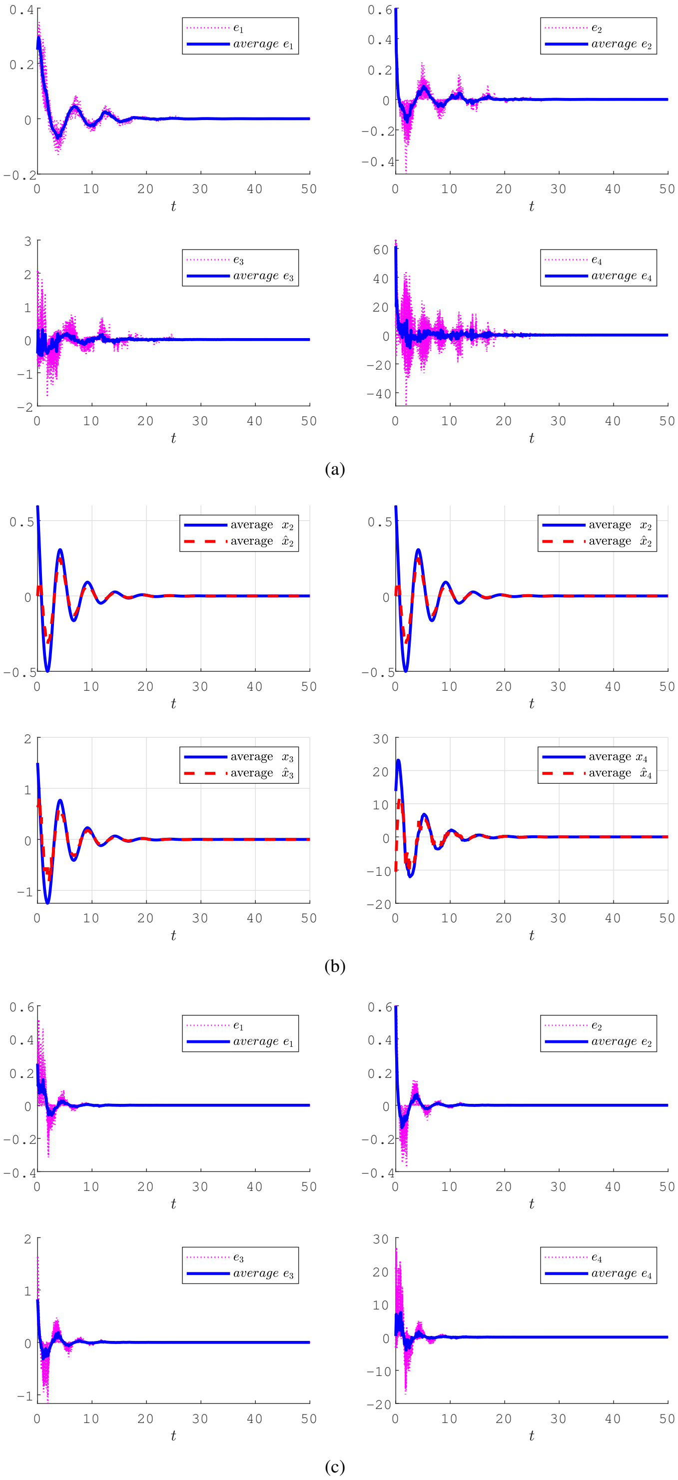

Fig. 7. Estimation error under 50 random independent trials.

[4] Y. Gao, F. Xiao, J. Liu, R. Wang, Distributed soft fault detection for interval type-2 fuzzy-model-based stochastic systems with wireless sensor networks, IEEE Transactions on Industrial Informatics 15 (1) (2019) 334–347.

[5] M. Kchaou, M. A. Regaieg, A. Al-Hajjaji, Quantized asynchronous extended dissipative observer-based sliding mode control for markovian jump (TS) fuzzy systems, Journal of the Franklin Institute 359 (17) (2022) 9636–9665.

[6] M. Kchaou, O. Alshammari, H. Jerbi, R. Abassi, S. Ben Aoun, An adaptive event-triggered filtering for fuzzy Markov switching systems with quantization and deception attacks: a non-stationary approach, International Journal of Fuzzy Systems 26 (6) (2024) 1879–1896.

[7] M. A. Regaieg, M. Kchaou, A. El-Hajjaji, M. Chaabane, Robust H_∞ guaranteed cost control for discrete-time switched singular systems with time-varying delay, Optimal Control Applications and Methods (2018) (2018).

[8] Z. Minjie, Z. Yujie, Y. Shenhua, L. Lina, Sampled-data control for nonlinear singular systems based on a $Takagi–Sugeno$ fuzzy model, Transactions of the Institute of Measurement and Control 40 (14) (2018) 4027–4036.

[9] H. Jerbi, M. Kchaou, O. Alshammari, R. Abassi, D. Popescu, Observer-based feedback control of interval-valued fuzzy singular system with time-varying delay and stochastic faults, International Journal of Computers, Communications & Control 17 (6) (2022) 1–23.

[10] B. T. Mourad Kchaou, Houssem Jerbi, A. Kouzou, Non-fragile mixed h_∞/passive-based asynchronous sliding mode control for nonlinear singular markovian jump systems, International Journal of Systems Science 53 (3) (2022) 447–467.

[11] Y. Yuan, H. Yang, L. Guo, F. Sun, Analysis and design of networked control systems under attacks, Crc Press, 2018.

[12] N. Zhao, P. Shi, W. Xing, C. P. Lim, Event-triggered control for networked systems under denial of service attacks and applications, IEEE Transactions on Circuits and Systems I: Regular Papers 69 (2) (2022) 811–820.

[13] H. Zhang, J. Hu, G.-P. Liu, X. Yu, Event-triggered secure control of discrete systems under cyber-attacks using an observer-based sliding mode strategy, Information Sciences 587 (2022) 587–606.

[14] Q.-X. Chen, X.-H. Chang, Resilient filter of nonlinear network systems with dynamic event-triggered mechanism and hybrid cyber attack, Applied Mathematics and Computation 434 (2022) 127419.

[15] B. Kaviarasan, O.-M. Kwon, M. J. Park, R. Sakthivel, Reduced-order filtering for semi-markovian jump systems against randomly occurring false data injection attacks, Applied Mathematics and Computation 444 (2023) 127832.

[16] J. Liu, T. Yin, J. Cao, D. Yue, H. R. Karimi, Security control for T-S fuzzy systems with adaptive event-triggered mechanism and multiple cyber-attacks, IEEE Transactions on Systems, Man, and Cybernetics: Systems 51 (10) (2021) 6544–6554.

[17] X. Cai, K. Shi, K. She, S. Zhong, Y. Tang, Quantized sampled-data control tactic for T-S fuzzy NCS under stochastic cyber-attacks and its application to truck-trailer system, IEEE Transactions on Vehicular Technology 71 (7) (2022) 7023–7032.

[18] J. Liu, Y. Gu, J. Cao, S. Fei, Distributed event-triggered H_∞ filtering over sensor networks with sensor saturations and cyber-attacks, ISA Transactions 81 (2018) 63–75.

[19] H. Yang, H. Han, S. Yin, H. Han, P. Wang, Sliding mode-based adaptive resilient control for markovian jump cyber–physical systems in face of simultaneous actuator and sensor attacks, Automatica 142 (2022) 110345.

[20] Y. Song, Z. Li, F. Li, R. Xia, H. Shen, H_∞ static output feedback control for singularly perturbed persistent dwell-time switched systems with time-varying delay and deception attacks, Mathematical Methods in the Applied Sciences 46 (4) (2023) 3783–3796.

[21] Y. Pan, Y. Wu, H.-K. Lam, Security-based fuzzy control for nonlinear networked control systems with dos attacks via a resilient event-triggered scheme, IEEE Transactions on Fuzzy Systems 30 (10) (2022) 4359–4368.

[22] F. Guo, M. Luo, J. Cheng, I. Katib, K. Shi, Non fragile observer-based event-triggered fuzzy tracking control for fast-sampling singularly perturbed systems with dual-layer switching mechanism and cyber-attacks, Chaos, Solitons & Fractals 175 (2023) 114029.

[23] J. Wang, C. Yang, J. Xia, Z.-G. Wu, H. Shen, Observer-based sliding mode control for networked fuzzy singularly perturbed systems under weighted try-once-discard protocol, IEEE Transactions on Fuzzy Systems 30 (6) (2022) 1889–1899.

[24] B. Jiang, Y. Kao, C. Gao, X. Yao, Passification of uncertain singular semi-markovian jump systems with actuator failures via sliding mode approach, IEEE Transactions on Automatic Control 62 (8) (2017) 4138–4143.

[25] J. Song, Z. Wang, Y. Niu, H. Dong, Genetic-algorithm-assisted sliding-mode control for networked state-saturated systems over hidden markov fading channels, IEEE Transactions on Cybernetics 51 (7) (2021) 3664–3675.

[26] O. Gonzales-Zurita, O. L. Andino, J.-M. Clairand, G. Escrivá-Escrivá, Pso tuning of a second-order sliding-mode controller for adjusting active standard power levels for smart inverter applications, IEEE Transactions on Smart Grid 14 (6) (2023) 4182–4193.

[27] L. Hu, W. Lei, J. Zhao, X. Sun, Optimal weighting factor design of finite control set model predictive control based on multiobjective ant colony optimization, IEEE Transactions on Industrial Electronics (2023) 1–11.

[28] S. Zhao, T. Zhang, S. Ma, M. Chen, Dandelion optimizer: A nature-inspired metaheuristic algorithm for engineering applications, Engineering Applications of Artificial Intelligence 114 (2022) 105075.

[29] R. Abbassi, S. Saidi, A. Abbassi, H. Jerbi, M. Kchaou, B. N. Alhasnawi, Accurate key parameters estimation of pemfc's models based on dandelion optimization algorithm, Mathematics 11 (6) (2023).

[30] J. Hu, Z. Wang, Y. Niu, H. Gao, Sliding mode control for uncertain discrete-time systems with markovian jumping parameters and mixed delays, Journal of the Franklin Institute 351 (4) (2014) 2185–2202.

[31] O. Alshammari, M. Kchaou, H. Jerbi, S. Ben Aoun, V. Leiva, A fuzzy design for a sliding mode observer-based control scheme of takagi-sugeno markov jump systems under imperfect premise matching with bio-economic and industrial applications, Mathematics 10 (18) (2022).

[32] H. Li, Y. Pan, Q. Zhou, Filter design for interval type-2 fuzzy systems with d stability constraints under a unified frame, IEEE Transactions on Fuzzy Systems 23 (3) (2015) 719–725.

[33] X. Gao, F. Deng, P. Zeng and H. Zhang, Adaptive Neural Event-Triggered Control of Networked Markov Jump Systems Under Hybrid Cyberattacks, IEEE Transactions on Neural Networks and Learning Systems, 34 (3) (2023) 1502–1512

[34] X. Sun and Q. . Zhang, Observer-Based Adaptive Sliding Mode Control for T-S Fuzzy Singular Systems, IEEE Transactions on Systems, Man, and Cybernetics: Systems, 50 (11) (2020) 4438–4446

[35] M. Kchaou and H. Jerbi Reliable H_∞ and Passive Fuzzy Observer-Based Sliding Mode Control for Nonlinear Descriptor Systems Subject to Actuator Failure. Int. J. Fuzzy Syst. 24 (2022) 105–120

[36] X. Sun, L. Zhang and J. Gu, Neural-network based adaptive sliding mode control for Takagi-Sugeno fuzzy systems, Information Sciences, 628 (2023)

[37] Lin X, Wang Y, Liu Y. Neural-network-based robust terminal sliding-mode control of quadrotor. Asian J Control, 24 (2022)427–438.

[38] J. Li and G. H. Yang, Fuzzy Descriptor Sliding Mode Observer Design: A Canonical Form-Based Method, IEEE Transactions on Fuzzy Systems 28 (9) (2020) 2048–2062.

[39] Y. Fu, D. Liu, J. Chen, L. He, Secretary bird optimization algorithm: a new metaheuristic for solving global optimization problems, Artificial Intelligence Review 57 (5) (2024) 123.

[40] N. Zhang, W. Qi, G. Pang, J. Cheng, K. Shi, Observer-based sliding mode control for fuzzy stochastic switching systems with deception attacks, Applied Mathematics and Computation 427 (2022) 127153.

[41] J. Li, H. Wang, Fuzzy switching function-based sliding mode controller design for t-s fuzzy descriptor systems, Information Sciences 624 (2023) 344–360.

[42] Z. Cao, Y. Niu, J. Song, Finite-time sliding-mode control of markovian jump cyber-physical systems against randomly occurring injection attacks, IEEE Transactions on Automatic Control 65 (3) (2020) 1264–1271.